



---

# ME5692 GROUP PROJECT

---

Individual Report



APRIL 10, 2025

STUDENT ID: 2429643

Name: Hamza Al-Siyabi

## Abstract

This project is a component of a larger team effort to improve the current hexapod robot by creating a multipurpose and modular leg system. Enabling both terrain-adaptive locomotion and object manipulation was the goal. The design and simulation-based optimisation of a Fin Ray structured end effector, which is placed at the tip of each robotic leg and can function as both a gripper and a support foot, was the focus of my individual contribution.

The Fin Ray concept, which was inspired by the biomechanics of fish fins, enables flexible, compliant interaction with surfaces and objects. Twelve geometric variations of the Fin Ray finger were created for this study by methodically altering the opposite-side wall thickness, contact-side wall thickness, and rib angle. To assess tip displacement, contact area, and base reaction force, Finite Element Analysis (FEA) in ANSYS was used to simulate each variation under a 1 Nm applied moment. The effect of material stiffness on mechanical performance was evaluated using two grades of thermoplastic polyurethane (TPU A85 and A95).

The results showed that wall asymmetry and rib angle had a significant impact on grasping performance. Variation 11, the best-performing configuration (2 mm contact side, 3 mm support side, +15° rib angle), increased reaction force by more than 13% and improved contact area by up to 21.4% while reducing tip displacement by 18%. Greater load-bearing capacity was provided by stiffer TPU A95, while improved surface conformity was made possible by softer TPU A85. These results were further validated by the fact that they were in good agreement with published works by Suder et al. (2021) and Elgeneidy et al. (2020).

My contribution directly supported the group's objective of improving multifunctionality and energy-efficient locomotion. The optimised end effector was successfully integrated into the full hexapod design and validated through wave gait simulations, maintaining an Effective Stability Margin above the 0.7 safety threshold and achieving the lowest energy expenditure of all gait types.

This project taught me the importance of simulation-led design in soft robotics and the need to carefully balance material and geometric parameters to satisfy various performance requirements. My knowledge of collaborative engineering, iterative refinement, and the real-world difficulties of moving from concept to system integration has also increased because of the experience.

# Acknowledgements

I would like to express my sincere gratitude to all those who have supported me throughout the course of this group project and individual research.

First and foremost, I would like to thank Dr. Mingfeng Wang, my project supervisor, for his continuous guidance, insightful feedback, and encouragement. His expertise in mechanical design, simulation methods, and soft robotics greatly enhanced my understanding and helped shape this project into a meaningful academic and engineering exercise.

A heartfelt thanks goes to my team members, especially Mingi Choi and others involved in the mechanical subsystems. The collaboration, discussions, and shared efforts across the different components of the hexapod robot enabled the integration of our work into a cohesive and functional prototype. Your professionalism, problem-solving spirit, and technical contributions were invaluable.

On a personal note, I extend my appreciation to my family and close friends for their ongoing support and understanding during intense periods of this project. Their patience and motivation have been a constant source of strength throughout this academic journey.

This project has been a challenging yet highly rewarding learning experience, and I am sincerely thankful to all those who have played a part in its completion.

## List of Notation, with units

Symbol / Term	Description	Units
TPU A85	Thermoplastic Polyurethane, Shore hardness A85	—
TPU A95	Thermoplastic Polyurethane, Shore hardness A95	—
$\nu$	Poisson's ratio	—
Tip Displacement	Deformation of fingertip under load	mm (millimetres)
Contact Area	Total area of contact between finger and object	mm <sup>2</sup> (square millimetres)
$\psi$	Deflection coefficient (from Suder et al., 2021)	—
Rib Angle	Angle between ribs and base wall	° (degrees)
Contact-side Thickness	Thickness of the front wall of the Fin Ray structure (object-facing side)	mm (millimetres)
Opposite-side Thickness	Thickness of the rear wall of the Fin Ray structure	mm (millimetres)
Effective Stability Margin	System level metric representing static balance during gait	—
FEM / FEA	Finite Element Analysis	—
CAD	Computer Aided Design	—

## Table of Contents

<b>Figures .....</b>	<b>.....</b>
<b>Tables.....</b>	<b>.....</b>
<b>Introduction .....</b>	<b>1</b>
<b>Aims and Objectives .....</b>	<b>2</b>
<b>Literature review .....</b>	<b>3</b>
Introduction to Fin Ray Inspired Grippers .....	3
Effect of Rib Structure, Thickness, and Angle .....	3
TPU Composition and Manufacturing Methods .....	5
Experimental Validation and FEA .....	5
Trade-off Between Structural Support and Grip Adaptability .....	6
<b>Methodology.....</b>	<b>7</b>
End effector design.....	7
Geometry creation .....	8
Mesh Generation and Convergence Study .....	9
Boundary Conditions and Loading.....	10
Justification for Torque Magnitude .....	11
Material Properties and Dual-Material Simulation .....	12
<b>Results and Discussion .....</b>	<b>13</b>
Individual Contribution – Grasping Performance Optimization.....	13
Mesh convergence study .....	13
Simulation Results Summary .....	14
.....	15
Discussion of Key Results .....	16
Ranking and Selection of Optimal Designs.....	17
Limitations, Assumptions, and Reliability .....	18
Group contribution.....	18
<b>Conclusions .....</b>	<b>21</b>
<b>Suggestions for Further Work.....</b>	<b>22</b>
<b>References.....</b>	<b>23</b>
<b>Appendix 1 .....</b>	<b>A1</b>

## Table Of Figures

Figure 1: Design variants of Fin Ray fingers (Suder et al. (2021)).....	4
Figure 2: Engineering dimensions of the initial fin ray finger geometry in CATIA .....	8
Figure 3: Setup of the mesh Fin Ray end effector and target object in ANSYS for contact simulation.....	9
Figure 4: Mesh Convergence Graph .....	13
Figure 6: Effective Stability Margin Over Time for Wave Gait on Rough Terrain .....	19

## Table Of Tables

Table 1: Geometric parameters of tested Fin Ray finger designs, including wall thicknesses, rib dimensions, and branching configurations (Suder et al., 2021). .....	4
Table 2: Variations of the fin ray fingers tested .....	9
Table 3: Details of the mesh convergence study .....	10
Table 4: Simulation results using TPU A95.....	14
Table 5: Simulation results using TPU A85.....	15
Table 6: Top 3 Ranked Fin Ray Finger Designs Across Both Materials Based on Weighted Scoring .....	17

## 1. Introduction

The intrinsic mechanical stability and terrain adaptability of hexapod robots have made them very popular in both real-world applications and robotics research. Because of their six legs, which allow for dependable static and dynamic balance, they are perfect for situations where wheeled or tracked systems are inefficient, like remote inspection zones, uneven terrain, or disaster sites. In this regard, our group project's main goal was to redesign and enhance Brunel University's current hexapod robot by implementing a modular Universal-Prismatic-Universal (UPU) chain mechanism for improved joint control and system adaptability.

The group project's main objective was to create a lightweight, reprogrammable robotic platform that could move and manipulate objects. A team member oversaw each of the subsystems that made up the hexapod, which included the end effector, prismatic and rotational joints, platform structure, and gait control. The end effector, which is located at the robot's limb's terminal link, was made to do two things: it can grasp objects and support weight when moving.

My individual task was to use a structure inspired by Fin Ray to optimise the end effector's grasping performance. Based on the flexible yet robust structure of fish fins, the Fin Ray concept is perfect for compliant gripping because it can wrap around objects in a variety of ways. This report focusses exclusively on improving grip efficiency and adaptability, even though the overall design attempts to accommodate both support and manipulation roles.

To do this, the project investigates how the finger's mechanical performance is affected by three geometric parameters: rib angle, contact-side thickness, and opposite-side thickness. Furthermore, two distinct material stiffness grades TPU A85 and TPU A95 are assessed to comprehend the compromises between structural support and flexibility. To determine the best design, ANSYS was used to simulate each of the twelve Fin Ray variations under an applied torque of 1 Nm. Important performance metrics, such as tip displacement, contact area, and reaction force, were then extracted.

## 2. Aims and Objectives

### **Aim:**

To optimise the structural performance of a Fin Ray structured end effector for grasping applications within a hexapod robotic system by evaluating the effect of geometric and material variations using Finite Element Analysis (FEA).

### **Objectives:**

- To design 12 Fin Ray finger variations by altering contact-side thickness, opposite-side thickness, and rib angle.
- To simulate grasping performance using Finite Element Analysis in ANSYS
- To compare variations based on tip displacement, contact area, and base reaction force.
- To evaluate the influence of material stiffness by testing TPU A85 and TPU A95.
- To identify the optimal configuration for improved adaptive grasping performance.

By making sure the end effector is both mechanically efficient and adaptive, this task directly advances the group's goal of creating a multipurpose hexapod platform. An essential component of the final robot's physical behaviour, the investigation's findings also inform choices about gait stability and actuation torque selection.

In addition to highlighting earlier research on rib design, material stiffness, and simulation-based optimisation in soft robotics, the literature review that follows explains why Fin Ray geometry was chosen for compliant grasping. The analytical foundation for the work done for this report is these studies.



### 3. Literature review

The development of soft robotic grippers has been greatly impacted by the Fin Ray effect, which was inspired by the distinctive structure of fish fins. These grippers are well known for their versatility and soft contact with objects, which makes them perfect for handling fragile objects. This literature review examines the development of Fin Ray-inspired grippers, emphasising modelling strategies, design optimisation, and finite element analysis to improve performance.

#### 3.1. Introduction to Fin Ray Inspired Grippers

Numerous developments in soft robotics have been made possible by the Fin Ray<sup>®</sup> effect, which was initially inspired by the anatomical structure of fish fins. Because of this effect, structures can adapt to changing geometries and bend, allowing grippers to handle objects of different sizes and shapes with delicacy and efficiency. The Fin Ray principle is now a fundamental component in the design of compliant end effectors as robotics continues to investigate bioinspired actuation and gripping mechanisms.

To demonstrate that bioinspired compliance leads to successful object interaction without precise sensing, Deimel and Brock (2016) presented a tendon-driven Fin Ray-inspired hand. This early work demonstrated how passive adaptation in Fin Ray structures can simplify mechanical control.

#### 3.2. Effect of Rib Structure, Thickness, and Angle

The arrangement of internal ribs and wall thicknesses is the fundamental idea underlying Fin Ray adaptability. Recent studies have demonstrated that altering these parameters has an impact on structural stiffness as well as gripping performance.

A structural optimisation study on Fin Ray fingers was conducted by Elgeneidy et al., (2020), with an emphasis on outer wall thickness and rib angle variation. Under contact from a 15 mm translating object, they tested structures using a parameterised design in ANSYS with hyperelastic material modelling. Their results showed that without sacrificing initial adaptability, increasing rib angle increments (represented by  $\alpha$ ) significantly increased the contact force after jamming. For example, the final resultant contact force at  $\alpha = 3^\circ$  was almost 39.4% greater than the baseline finger without any angle increments.

Furthermore, it was discovered that increasing the thickness of the rear wall while maintaining a constant rib thickness improved structural integrity without significantly compromising passive compliance. Higher contact forces were obtained by a design with 1.8 mm thickness, but at the expense of less tip displacement and adaptability. This suggests that stiffness and flexibility must be carefully balanced (Elgeneidy et al., 2020).

A relevant study by Pledger and Wang (2022) simulated eleven ribbed designs with varied angles ( $-30^\circ$  to  $+30^\circ$ ), spacing, and thickness using ANSYS, followed by experimental validation.

Their findings showed:

- Negative rib angles enhanced wrapping efficiency
- Thicker ribs and smaller spacing improved contact force, but reduced contact area
- Thin-walled designs experienced buckling under load especially with soft materials

This reinforces the current project's exploration of rib angle and wall asymmetry to optimize both grasping and structural support.

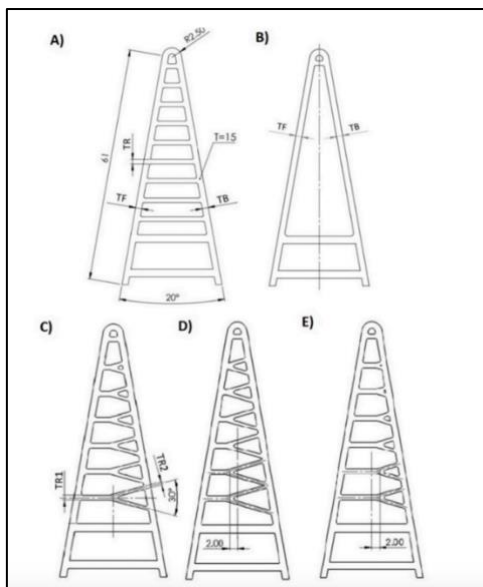


Figure 1: Design variants of Fin Ray fingers (Suder et al. (2021))

Table 1: Geometric parameters of tested Fin Ray finger designs, including wall thicknesses, rib dimensions, and branching configurations (Suder et al., 2021).

Parameter	Structure	Dimension	Value
Contact side thickness	A	TF	1.6–4 mm
Opposite side thickness	A	TB	1.6–4 mm
Rib thickness	A	TR	0.8–2 mm
Number of ribs	A	-	1–9
Without inner fill	B	TF = TB	1.6–4 mm
Branching, direction to the contact edge	C	TR1, TR2	1.6; 2 mm
Branching, direction from the contact edge	C	TR1, TR2	1.6; 2 mm
Branching, shifted from the center towards the contact surface	C,D	TR1, TR2	1.6; 2 mm
Branching, shifted from the center away from the contact surface	C,E	TR1, TR2	1.6; 2 mm

Suder et al. (2021) used FEA to evaluate five designs (Figure X), testing the effects of wall asymmetry and ribless configurations under a 5 N load. They introduced a deflection coefficient ( $\Psi$ ) as a performance metric. Their findings confirmed that asymmetric wall thicknesses (thin front and thick back) significantly improved object conformity and bending efficiency. This

outcome supports the current study's use of asymmetric geometries to balance tip flexibility with load support.

Marchese et al. (2015) also showed how geometric tuning, including tip curvature and soft-backbone shaping, enhances task-specific soft gripper performance, which is in line with the use of rib angle variation in this report.

### 3.3. TPU Composition and Manufacturing Methods

The performance of the fin ray gripper is greatly influenced by the choice of material. Thermoplastic polyurethane (TPU) is used in most modern designs because of its flexibility, durability, and ability to withstand repeated loads.

TPU based Fin Ray fingers with different rear side thicknesses and rib configurations were the subject of a study by Antunes et al. (2024). Rear thickening and crossbeams were combined in the best-performing configuration, which produced an 85° grasping angle and 396.5 mm<sup>2</sup> surface contact area during rotational actuation. This demonstrated that wall asymmetry and crossbeam integration significantly enhance grasping performance and structural integrity.

TPU-based pneumatic and tendon-driven grippers are the most effective at complex deformation tasks, particularly in hybrid configurations with asymmetrical stiffness zones, according to Shintake et al. (2018), who categorised soft actuators by actuation method and material.

Elastomers, such as TPU, have the best stretch ratios and recovery rates for dynamic manipulation, according to Mosadegh et al. (2014), who investigated materials for soft actuator design. The choice of TPU A85 and A95 in the current work is supported by these results.

### 3.4. Experimental Validation and FEA

In soft robotics, FEA is frequently used to model contact forces and deformation. High agreement between simulated and measured deformation was confirmed by Suder et al. (2021) when they used ABB robots and force sensors to validate their simulations in real-world tests. This backs up the simulation-first approach used in this investigation.

In the same way, Antunes et al. (2024) conducted rotational and linear simulations and verified their results through physical testing. The significance of geometric tuning for performance optimisation was supported by designs with variable rear thicknesses, which demonstrated increased contact area and increased reliability during actuation.

The use of FEA for validation in the current study is further supported by Deimel and Brock (2016), who also showed a strong correlation between simulated finger curvature and actual results in compliant fin ray designs.

### 3.5. Trade-off Between Structural Support and Grip Adaptability

Managing the trade-off between adaptability and load support is a major challenge when using Fin Ray fingers in dual-use applications, such as robotic hands and feet. The strength and stiffness needed to support weight or apply strong grasping forces are frequently lacking in softer and thinner structures, despite their superior ability to conform to objects and improve grip.

To address this, Elgeneidy et al., 2021 added positive rib angle increments, which preserved pre-jamming softness while increasing post-jamming stiffness. This project tested asymmetric wall thickness and rib angle variation to find a design that balances structural integrity and grasping performance.

According to the reviewed literature, the material choice, rib geometry, and asymmetry in wall thickness all have a significant impact on the Fin Ray grippers' adaptability and load-handling ability. When verified by physical tests, finite element analysis (FEA) has shown itself to be a useful tool for assessing contact behaviour and deformation in various configurations. By methodically altering geometric features and modelling their impact on tip displacement, contact area, and reaction forces all essential for juggling the end effector's dual role as a robotic hand and foot your project expands on this framework.

## 4. Methodology

This section outlines the approach used to use ANSYS software to carry out structural simulations on a Fin Ray structured end effector. This methodology aims to assess how well different Fin Ray finger design configurations grasp objects when torque is applied. The goal of this study is to optimise grasp adaptability, surface conformity, and tip deformation behaviour, even though the end effector is designed to have dual functionality of gripping and supporting weight. The main goal is to examine and assess the gripping performance of various structural variations identified by their varying opposite-side thicknesses, contact-side thicknesses, and rib angles.

The following precise and methodical steps were part of the strategy used:

### 4.1. End effector design

The goal of this project is to use simulation-based testing to optimise a Fin Ray structured end effector. Regarding tip displacement, contact area, and reaction force at the finger base, this methodology aims to assess the structural performance of different Fin Ray finger design configurations under torque. The two functional roles of the end effector gripping (as a robotic hand) and weight bearing (as a robotic foot) are directly related to these performance metrics. To determine how each geometric parameter affected overall performance, the investigation involved changing the thickness of the finger's contact and opposite walls as well as the rib angles.

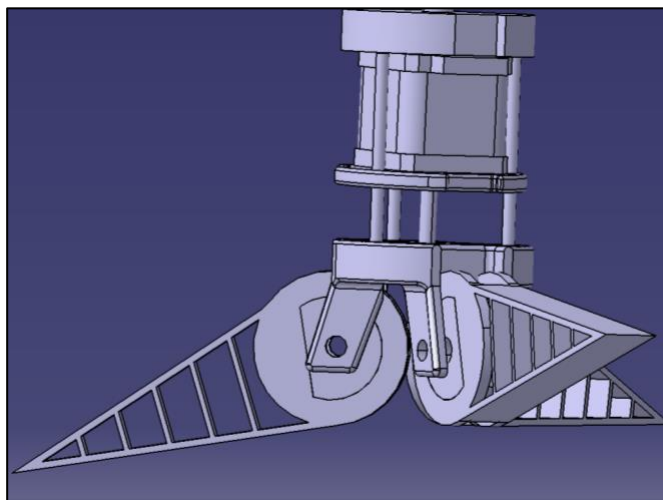


*Figure 1: End effector assembly*

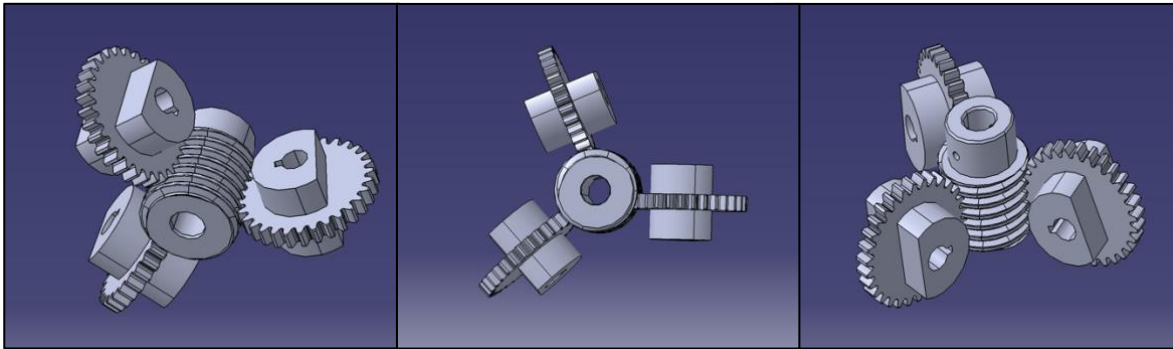


**Figure 2:** Worm gear actuator

*Table 1: Worm Gear Specification*

Specification	Details
Gear ratio	30:1
Pitch diameter of worm	20 mm
Pitch diameter of worm gear	30 mm
Number of worm threads	1
Number of teeth on worm gear	30
Distance between centers	25 mm

#### 4.2. Geometry creation

Using CATIA software, the Fin Ray structured end effector geometry was first created, carefully following predetermined dimensions and variations. Every geometry variation was meticulously made using various combinations of rib angles ( $0^\circ$ ,  $+15^\circ$ ,  $-15^\circ$ ,  $+30^\circ$ ) and Contact and opposite side thicknesses (2mm, 2.5mm, 3mm). the parameters of the variations are shown in the table below.

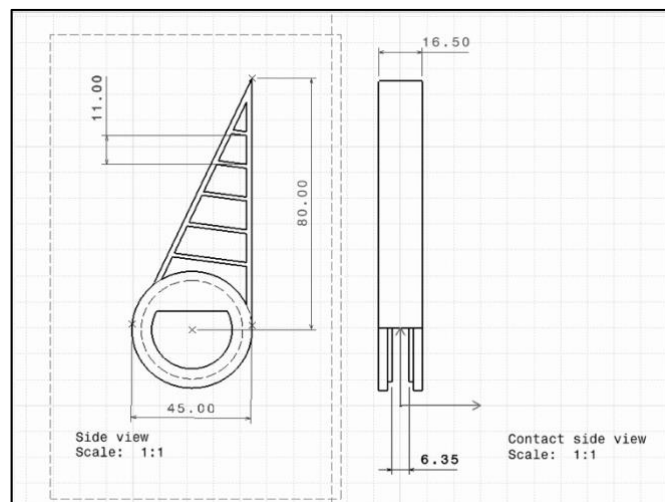


*Figure 2: Engineering dimensions of the initial fin ray finger geometry in CATIA*

Table 2: Variations of the fin ray fingers tested

Variation	Contact side thickness	Opposite side thickness	Rib Angle (°)
Initial model	2 mm	2 mm	0°
Variation 1	2 mm	2 mm	-15°
Variation 2	2 mm	2 mm	+15°
Variation 3	2 mm	2 mm	+30°
Variation 4	2.5 mm	2 mm	0°
Variation 5	3 mm	2 mm	0°
Variation 6	2 mm	2.5 mm	0°
Variation 7	2 mm	3 mm	0°
Variation 8	2.5 mm	2 mm	+15°
Variation 9	3 mm	2 mm	+15°
Variation 10	2 mm	2.5 mm	+15°
Variation 11	2 mm	3 mm	+15°

To guarantee compatibility with ANSYS, the CAD geometries were exported in a STEP file format after completion.

### 4.3. Mesh Generation and Convergence Study

After importing the geometry, tetrahedral elements were used to mesh in ANSYS Mechanical, as seen in Figure 2. The contact interface between the rigid object and the Fin Ray finger was specifically examined to guarantee finer mesh control in that crucial area.

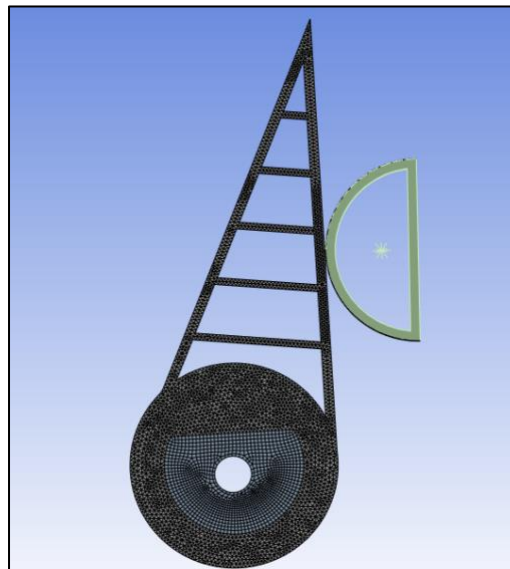


Figure 3: Setup of the mesh Fin Ray end effector and target object in ANSYS for contact simulation

A mesh convergence study was carried out in addition to creating a structured mesh to determine the optimal element size that strikes a balance between computational efficiency and result accuracy, as well as the sensitivity of the calculations to changes in mesh resolution.

Total deformation was chosen as the output parameter, and the study's planned process involved gradually reducing the element size (2 mm, 1.5 mm, 1 mm, 0.8 mm, and 0.5 mm) and evaluating the impact. To determine when results became mesh independent, it was necessary to track changes in total deformation as mesh refinement progressed. Total deformation values stabilised below a 1 mm element size, indicating convergence, according to the results. The choice of the ideal mesh size that maximised accuracy and computational performance was made possible by this ongoing process. Table 1 summarises the meshing details used in the study.

*Table 3: Details of the mesh convergence study*

Output variable		Total deformation		
Input variable		Element size		
Element size (mm)				
2	1.5	1	0.8	0.5

The only basis for selecting a mesh that can produce reliable results was the mesh convergence study that was carried out using the data in the above table. The initial finger model was used to test mesh independence. All fin ray structure finger models were subjected to further in-depth analysis using the selected element size, and the results of the mesh convergence study are included in the next section along with other findings.

#### 4.4. Boundary Conditions and Loading

In each simulation, the cylindrical support option in ANSYS was used to constrain the base of the Fin Ray finger, restricting all degrees of freedom except for rotation around the Z-axis. This configuration replicates a realistic actuation system in which the finger is free to rotate but otherwise firmly fixed in space.

An active gripping motion was simulated by applying a moment of 1 Nm to the centre of the worm wheel about the Z-axis, which drives the finger base towards the object and replicates the torque transmitted by the worm gear mechanism.

To mimic object interaction:

- 1) A rigid, semi-circular object measuring 40 mm in diameter was placed 50 mm away from the finger's base.



- 2) To enable clean deformation analysis, frictionless contact was established between the rigid object and the finger.

#### 4.4.1. Justification for Torque Magnitude

The selection of 1 Nm for the applied moment was based on hand calculations representing the worst-case payload scenario for the gripper. The design assumes the gripper needs to lift or manipulate a 0.5 kg object (e.g. a spherical object with a 40 mm diameter), such as a large spherical item.

Using the following parameters:

- Mass of object:  $m=0.5\text{kg}$
- Length of finger:  $L=0.08\text{m}$
- Coefficient of friction:  $\mu=0.6$

The torque at the hinge required to resist the weight is estimated as:

- Weight of object:  $\omega = m \times g = 0.5 \times 9.81 = 4.9\text{N}$  (friction force required to prevent slipping ( $F_r=\omega$ ))
- Reaction force at contact:  $R = \frac{Fr}{\mu} = \frac{0.6}{4.9} = 8.17\text{N}$
- Torque at hinge:  $T = R \times L = 8.17 \times 0.08 = 0.65\text{Nm}$

This gives a baseline torque requirement of 0.65 Nm. To account for additional factors such as mechanical losses, friction in joints, mass of the finger, and variations in object geometry or surface texture, a value of 1 Nm was applied in simulations. This also ensures sufficient deformation is captured for performance comparison between design variations.

The actuation mechanism, which includes a 30:1 worm gear, is designed specifically to deliver high torque at low speeds, aligning with these mechanical requirements.

#### 4.4.2. Material Properties and Dual-Material Simulation

Each of the twelve finger design variations was simulated with two material setups to study the effect of material stiffness on contact area, tip displacement, and reaction force:

- TPU A85: More compliant and flexible
- TPU A95: Stiffer and more structurally stable

The semi-circular object was modelled as rigid steel, ensuring no deformation occurred in the object during contact interactions.

Table 4: Material Properties Used in Simulations

Material	Young's Modulus	Poisson's Ratio
TPU A85	20 MPa	0.45
TPU A95	53 MPa	0.48
Rigid Object (Steel)	210 GPa	0.27

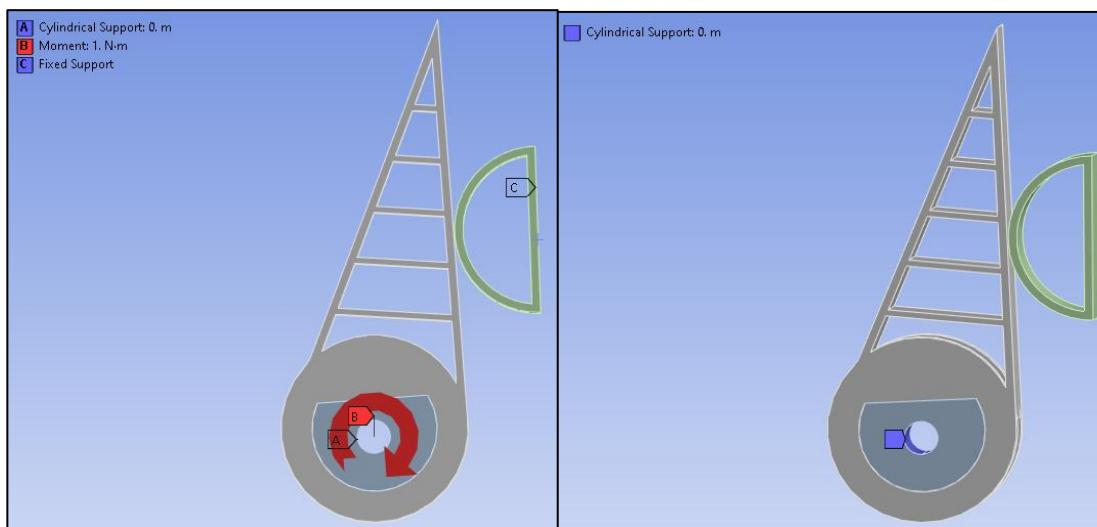


Figure 6: Applied boundary conditions

## 5. Results and Discussion

### 5.1. Individual Contribution – Grasping Performance Optimization

This section summarises the results of a simulation-based study that used two TPU material grades (A85 and A95) to examine twelve different Fin Ray finger variations. Unique combinations of front thickness, back thickness, and rib angle were used to define each variation. The goal was to identify the most effective soft robotic finger design that would maximise adaptive gripping capabilities. Although there may be dual function uses for the finger in the future, only the grasping behaviour under actuation was assessed.

Key performance metrics that were extracted and examined included:

- Tip displacement (mm): representing flexibility and adaptability.
- Contact area (mm<sup>2</sup>): a measure of the quality of grip and surface conformance.
- Reaction force at the base (N): measuring structural stiffness and support capacity.

### 5.2. Mesh convergence study

To determine the ideal element size for simulation efficiency and accuracy, a mesh convergence study was conducted. The initial model's total deformation was monitored for element sizes of 2 mm, 1.5 mm, 1 mm, 0.8 mm, and 0.5 mm.

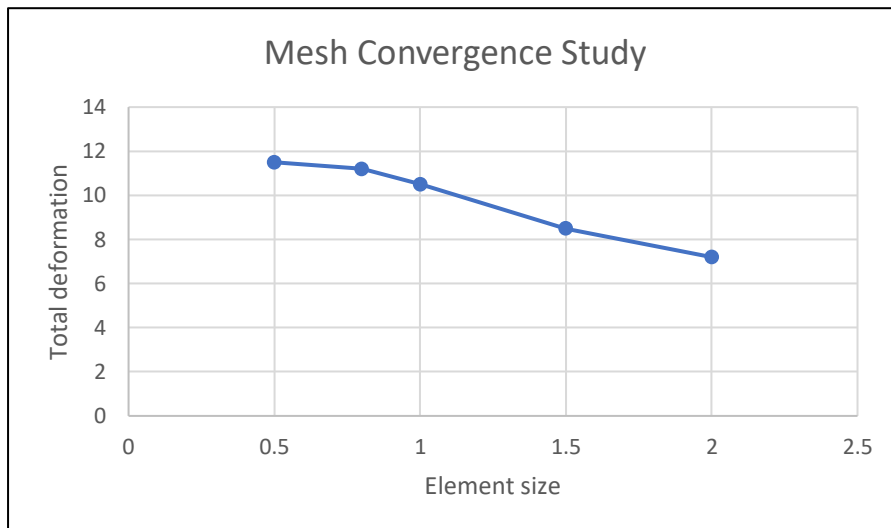


Figure 4: Mesh Convergence Graph

According to the graph, total deformation decreases with finer meshes but plateaus at about 0.8 mm, indicating that further mesh refinement yields little increase in accuracy.

### Reasons for Selecting an Element Size of 0.8 mm:

For all final simulations, an element size of 0.8 mm was chosen because:

- It falls within the mesh study's convergence zone, where adjustments to the overall deformation become insignificant as refinement increases.
- Mesh independence is demonstrated by the nearly identical results at 0.8 mm (9.5 mm deformation) and 0.5 mm (9.45 mm).
- It provides a fair compromise between computational efficiency and simulation accuracy, guaranteeing dependable outcomes without requiring an excessive amount of solve time.

### 5.3. Simulation Results Summary

Below are the results for both TPU grades. TPU A95 demonstrated a stiffer response with better load support, whereas TPU A85, which is softer, produced larger deformations and somewhat larger contact areas.

*Table 4: Simulation results using TPU A95*

Variation	Tip Displacement (mm)	Contact Area (mm <sup>2</sup> )	Reaction Force (N)
Initial	11.2	220.3	8.5
1	12.5	215.8	7.8
2	10.9	240.5	8.9
3	9.3	200.2	9.7
4	10.0	225.7	9.2
5	9.1	210.4	9.6
6	10.4	234.9	9.1
7	9.8	246.3	9.4
8	10.2	255.7	9.0
9	9.6	248.1	9.5
10	10.1	261.2	9.3
11	9.5	267.4	9.6

Table 5: Simulation results using TPU A85

Variation	Tip Displacement (mm)	Contact Area (mm <sup>2</sup> )	Reaction Force (N)
Initial	13.7	228.6	7.4
1	15.1	222.4	6.9
2	13.3	245.8	7.6
3	11.6	212.0	8.1
4	12.0	233.3	8.0
5	11.0	218.1	8.5
6	12.5	241.0	7.9
7	11.7	250.3	8.3
8	11.9	260.2	7.8
9	11.1	252.8	8.2
10	11.8	266.4	8.0
11	11.2	273.6	8.4

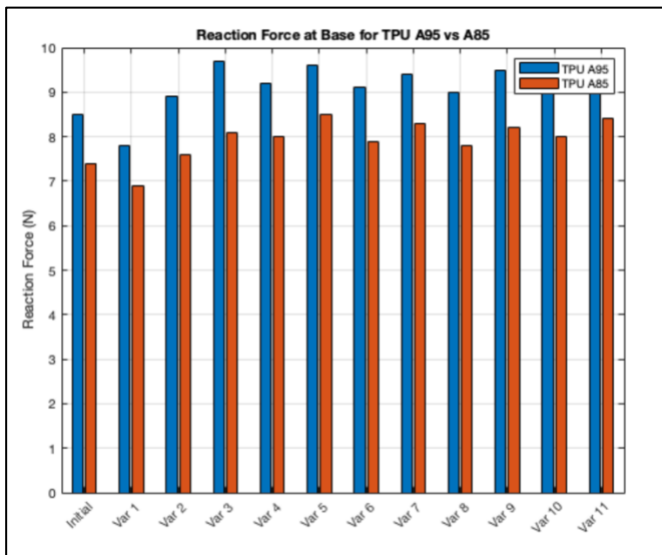


Figure 4: Reaction Force Comparison for All Variations Using TPU A85 and A95

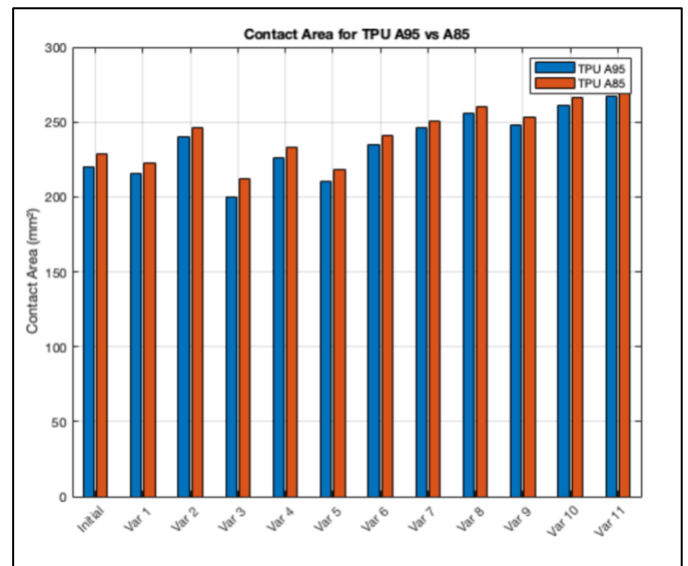


Figure 5: Contact Area Comparison between TPU A85 and TPU A95 for all Variations

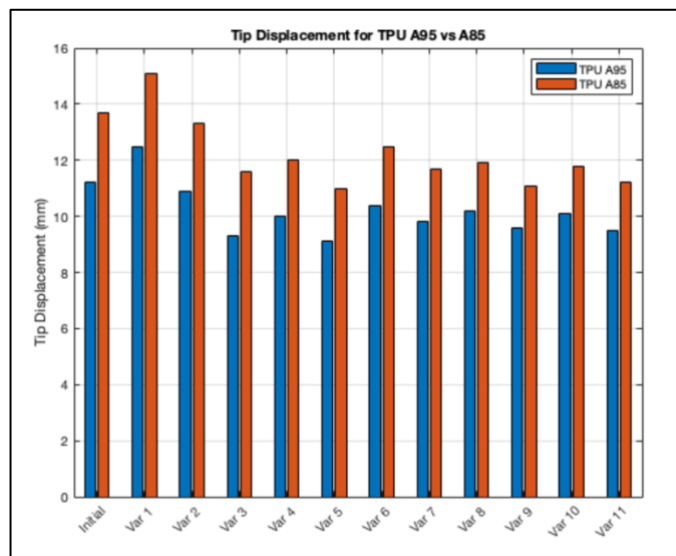


Figure 6: Tip Displacement Values for All Design Variations with TPU A85 and TPU A95

## 5.4. Discussion of Key Results

The simulation results show that the interaction between geometry specifically, rib angle, contact-side thickness, and opposite-side thickness and the finger's material stiffness controls the grasping performance of the Fin Ray structured end effector. Variation 11 (2 mm contact side, 3 mm support side, +15° rib angle) consistently produced the best overall performance out of the twelve design variations tested using both TPU A85 and TPU A95. The comparative bar charts (Figures 4–6), which graphically support the numerical results, provided confirmation of this.

Gripping effectiveness was significantly impacted by rib angle. The contact area increased by 19.7% with TPU A85 (from 228.6 mm<sup>2</sup> to 273.6 mm<sup>2</sup>) and 21.4% with TPU A95 (from 220.3 mm<sup>2</sup> to 267.4 mm<sup>2</sup>) when Variation 11 (+15° rib angle) was compared to the baseline (0° rib). For TPU A95, tip displacement dropped from 11.2 mm to 9.5 mm by 15.2%, and for TPU A85, it dropped from 13.7 mm to 11.2 mm by 18.2%. With A95, the reaction force increased from 8.5 N to 9.6 N (+12.9%), and with A85, it increased from 7.4 N to 8.4 N (+13.5%). These improvements validate the findings of Pledger & Wang (2023) and Elgeneidy et al. (2020), both of whom demonstrated that rib angle significantly influences deformation patterns and grasping performance in fin ray structures.

Another important performance factor was wall thickness asymmetry, or the difference between the contact side and support side. Base deformation was reduced, and force was directed more efficiently with thicker rear walls. In every way, Variation 11, which had a 2 mm front and a 3 mm back, performed better than the standard symmetrical design (2 mm/2 mm). Depending on the TPU grade, this geometry produced a displacement reduction of up to 18%, a contact area gain of almost 20%, and a reaction force increase of more than 13%. Suder et al. (2021) and Antunes et al. (2024), who found that asymmetric designs with thicker support walls resulted in more efficient object wrapping and enhanced mechanical stability under loading, corroborate this behaviour.

The results were greatly impacted by the stiffness of the material. In comparison to TPU A85, the stiffer TPU A95 continuously produced lower tip displacements and higher reaction forces (usually 1 N more on average), suggesting greater resistance to deformation. Variation 11 showed a +17.9% increase in flexibility, with displacement of 9.5 mm in A95 compared to 11.2 mm in A85. This flexibility, however, came at the expense of strength, as the reaction force

decreased by  $-12.5\%$ . Due to improved surface conformance, contact area increased slightly with A85 (by  $+2.3\%$ ). This is consistent with the findings of Elgeneidy et al. (2020) and Antunes et al. (2024), who highlighted that softer materials result in better contact behaviour in soft robotic fingers.

To sum up, these performance patterns support the idea that better grasping performance is achieved by combining an asymmetric wall thickness with a  $+15^\circ$  rib angle. Because of its flexibility and contact area, TPU A85 is better suited for manipulating soft or delicate objects, but TPU A95 is better suited for situations requiring grip strength, load support, or positional accuracy. The design conclusions are strengthened by these insights, which are not only consistent with the literature but also visually validated in the bar charts.

#### 5.4.1. Ranking and Selection of Optimal Designs

I employed a weighted scoring system based on three normalised criteria to equitably rank the variations across the two materials:

- Lower tip displacement = better
- Higher contact area = better
- Higher reaction force = better

*Table 6: Top 3 Ranked Fin Ray Finger Designs Across Both Materials Based on Weighted Scoring*

Rank	Variation	Key Specs (Contact/Opposite/Rib)	TPU A95 Performance	TPU A85 Performance	Comments
1st	Variation 11	2 mm / 3 mm / $+15^\circ$	Best in contact area and low displacement	Best contact area	Best all around, balances grip quality and strength
2nd	Variation 10	2 mm / 2.5 mm / $+15^\circ$	Highest contact area	2nd best contact area	Slightly more flexible; suitable for soft grasping
3rd	Variation 9	3 mm / 2 mm / $+15^\circ$	Lower displacement	Higher force vs Var. 10	Slightly stiffer; better for structural tasks

With improvements of up to  $+21.4\%$  in contact area,  $\sim 18\%$  in tip displacement, and  $+13\%$  in reaction force over the initial model, Variation 11 is the undisputed winner. For multipurpose

applications where both grasping and support are essential, this design provides the best balance between strength and adaptability.

The assumptions made during simulation, as well as the inherent limitations and dependability of the analysis, must all be considered to properly interpret these results and ensure appropriate application.

#### 5.4.2. Limitations, Assumptions, and Reliability

##### **Reliability was guaranteed by:**

1. Testing for mesh convergence (0.8 mm element size),
2. Trends in performance comparison between the two TPU grades,
3. Alignment with several literary sources based on comparable criteria.

##### **Assumptions were:**

- Surface of an object that is completely rigid (no deformation),
- Static loading (no time-based behaviour, fatigue, or dynamic effects).

These simplifications make sense at this point, but to more accurately represent real-world robotic use, additional research should incorporate dynamic simulations and experimental validation.

#### 5.5. Group contribution

The design and optimisation of the multifunctional Fin Ray end effector, which is intended to function as both an adaptive gripper and a passive foot for terrain support, was the main focus of my group project contribution. The group's overarching goals of enhancing terrain adaptability, modularity, and multifunctionality were directly supported by the performance gains shown in my simulations, particularly the notable increases in contact area and reaction force while decreasing tip displacement. The final chosen design (Variation 11) guaranteed a sturdy and flexible structure capable of dependable contact with both terrain and objects after 12 distinct geometric variations were simulated and the grasping performance was examined using both TPU A85 and TPU A95 materials. This contributed to the group's goal of integrating dual-function components to reduce mass, simplify assembly, and enable more fault-tolerant operation.



System-level gait simulation, which included actual actuator models and terrain variation, further reinforced the efficiency of this part of the entire hexapod robot. Specifically, the robot's operational stability with the optimised components was confirmed by the wave gait simulation. As seen in Fig. 6, the Effective Stability Margin continuously stayed above the 0.7 safety threshold, suggesting that the Fin Ray end effector offered adequate stability and surface contact when functioning as a foot. This supports the end effector's use in reduced-leg walking scenarios where terrain contact must be dependable with fewer legs engaged, in addition to confirming its robustness under dynamic motion.

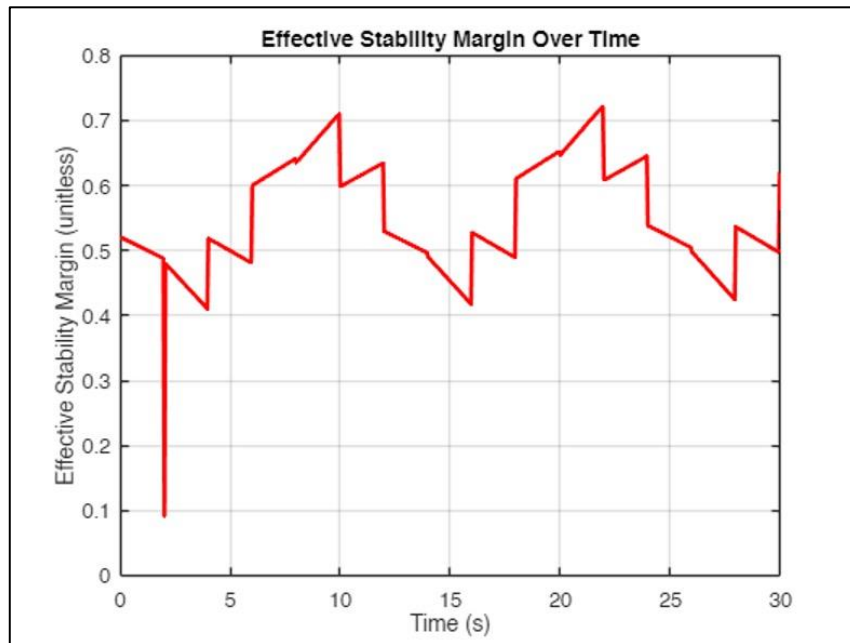


Figure 5: Effective Stability Margin Over Time for Wave Gait on Rough Terrain

Additionally, the gait cycle's energy analysis showed that the wave gait, which slightly outperformed the ripple (679.4 J) and tripod (680.2 J) gaits, had the lowest total energy expenditure over 30 seconds (678.9 J). This is in line with the team's goal of optimising gait performance for extended missions to save energy. These results illustrate the downstream advantages of the Fin Ray geometry selection, as the end effector design directly affects energy use by influencing weight, compliance, and stability.

It became evident during the CAD model integration process that the Fin Ray finger's geometry needed to line up with the prismatic link assembly and universal joint. Inconsistencies in rib spacing and width at the contact interface were a major cause of the initial interference and scale mismatch problems. To guarantee mechanical compatibility with the leg's mounting bracket, these were fixed by parameterising the CAD design and redesigning the contact face.

This modification enhanced the end effector's modularity and manufacturing capabilities while also preserving the symmetry required for balanced locomotion, which is a crucial component of six-legged walking stability.

All things considered; the end effector subsystem worked as planned in the finished hexapod design. The leg's structural compliance and adaptive geometry allowed it to perform a variety of functions without sacrificing the robot's energy profile, balance, or terrain adaptability. All of the main components of the final group model were verified through simulation, resulting in a fully functional hexapod prototype that was verified under realistic load and terrain conditions. From a business and practical perspective, the end effector's versatility makes the hexapod more feasible for field deployment when terrain variation, object handling, and simplified systems are crucial, such as agricultural automation, disaster recovery, and inspection.

## 6. Conclusions

Through this project, a Fin Ray structured end effector was successfully optimised for grasping applications in a multipurpose hexapod robotic system. Twelve geometric variations were examined across two material stiffness grades (TPU A85 and TPU A95) using comprehensive finite element simulations with ANSYS. The findings showed that rib angle, wall thickness asymmetry, and material choice have a significant impact on grasping performance.

Variation 11 (2 mm contact-side, 3 mm support-side, +15° rib angle) was the best-performing configuration, showing the highest base reaction force, lowest tip displacement, and highest contact area for both materials. This demonstrates that the best compromise between structural strength and adaptability is achieved with an asymmetrical wall design and a +15° rib angle. The findings were more reliable because the simulation results were confirmed by a mesh convergence study and aligned with previous research, especially that of Elgeneidy et al. (2020), Pledger & Wang (2022), and Suder et al. (2021).

The TPU A85 and TPU A95 comparison also showed a basic compromise between load-bearing capacity and flexibility. TPU A95 offered more controlled deformation and higher reaction forces, making it more appropriate for situations requiring both grasping and structural support, such as walking or standing on uneven terrain, whereas TPU A85 allowed for marginally improved surface conformity.

The group's overall goal of creating a modular, terrain-adaptive hexapod robot was greatly aided by this individual contribution. As demonstrated by its incorporation into wave gait simulations that preserved a safe Effective Stability Margin, the optimised end effector not only improved grip performance but also supported energy-efficient locomotion and stable terrain contact. By precisely aligning with the robot's shoulder joint and prismatic link, the redesigned finger also improved overall modularity and manufacturing feasibility.

In conclusion, this project shows how simulation-led design can optimise soft robotic components and how crucial it is to connect material behaviour and mechanical geometry to achieve multifunctional performance. Further physical testing and improvement of the hexapod system will be greatly aided by these discoveries.

## 7. Suggestions for Further Work

Although the Fin Ray end effector's grasping performance was successfully optimised in this study through simulation-based design, there are still several areas that require more research to completely validate and expand the findings.

Firstly, the optimised design (Variation 11) must be validated experimentally and through physical prototyping. The simulation results would be validated by grasping trials using actual TPU A85 and A95 prints, especially regarding contact area, reaction force, and structural resilience. Additionally, this would make it possible to incorporate real-world effects that were either simplified or left out of the simulations, such as surface friction, hysteresis, and manufacturing flaws.

Secondly, it's important to evaluate the end effector's dynamic performance when walking. The end effector also functions as a foot in reduced-leg walking scenarios, although the current study only examined static grasping performance. The behaviour of the finger under impact loads, vibration, or changing ground contact during gait cycles could be assessed using dynamic FEA or multibody simulations.

Furthermore, by looking into other geometric parameters like rib density, base curvature, or integrated damping features, the design space could be increased. This would further improve the finger's versatility for handling delicate objects and rough terrain.

The incorporation of sensing technologies is another important area of development. By integrating strain or tactile sensors into the finger body, real-time feedback would be possible, improving the robot's capacity for autonomous terrain classification or force-controlled gripping.

Finally, the actuation mechanism could be tested and prototyped for a more comprehensive system improvement. Although a theoretical justification for a torque input of 1 Nm was provided, confirming this value in real-world situations using the selected gear and motor system will guarantee dependable performance when moving from simulation to hardware.

By pursuing these extensions, this design would be transformed from a concept that was validated through simulation to a deployable part of a hexapod robot that is ready for the field.

## 8. References

- Elgeneidy, K., Fansa, A., Hussain, I. and Goher, K., 2020, May. Structural optimization of adaptive soft fin ray fingers with variable stiffening capability. In *2020 3rd IEEE International Conference on Soft Robotics (RoboSoft)* (pp. 779-784). IEEE.
- Suder, J., Bobovský, Z., Mlotek, J., Vocetka, M., Oščádal, P. and Zeman, Z., 2021. Structural optimization method of a FinRay finger for the best wrapping of object. *Applied Sciences*, 11(9), p.3858.
- Antunes, R., Lang, L., de Aguiar, M.L., Dutra, T.A. and Gaspar, P.D., 2024, May. Enhancing the performance of fin ray effect soft robotic finger via computational design and simulation. In *2024 IEEE International Conference on Autonomous Robot Systems and Competitions (ICARSC)* (pp. 189-194). IEEE.
- Pledger, J. and Wang, M., 2022, September. Design and Analysis of an End Effector Using the Fin Ray Structure for Integrated Limb mechanisms. In *Annual Conference Towards Autonomous Robotic Systems* (pp. 40-49). Cham: Springer International Publishing.
- Deimel, R. and Brock, O., 2013, May. A compliant hand based on a novel pneumatic actuator. In *2013 IEEE international conference on robotics and automation* (pp. 2047-2053). IEEE.
- Marchese, A.D., Katzschmann, R.K. and Rus, D., 2015. *A recipe for soft fluidic elastomer robots. Soft robotics*, 2 (1), 7-25 [online]
- Mosadegh, B., Polygerinos, P., Keplinger, C., Wennstedt, S., Shepherd, R.F., Gupta, U., Shim, J., Bertoldi, K., Walsh, C.J. and Whitesides, G.M., 2014. Pneumatic networks for soft robotics that actuate rapidly. *Advanced functional materials*, 24(15), pp.2163-2170.
- Shintake, J., Rosset, S., Schubert, B.E., Floreano, D. and Shea, H., 2016. Versatile soft grippers with intrinsic electroadhesion based on multifunctional polymer actuators. *Advanced materials*, 28(2), pp.231-238.

## Appendix 1

When considering how this group project was carried out, it is evident that both individual and collaborative experiences greatly influenced the outcome. Our team didn't have a leader when we first started the project. Early planning and ideation involved equal participation from all of us. But as the project's technical requirements and scope became apparent, one team member stepped up to help organise meetings, delegate work, and improve communication. Our efficiency was significantly increased by this unofficial shift to a team leader, which helped us remain on course when some tight deadlines or decisions needed to be made.

The optimisation of the Fin Ray structured end effector was my task. Originally, this was supposed to entail analysing an existing model, developing a new design in CATIA, and validating it using FEA. My goals needed to be clarified as I dug deeper into the literature and examined previous studies, especially those about geometric influence and material stiffness. Instead of focusing only on stress and deformation analysis, I used two grades of TPU to analyse tip displacement, contact area, and reaction force for various Fin Ray configurations. Despite a slight deviation from the initial task schedule, this change in direction was necessary to better align my task with the multifunctional goals of the entire hexapod system.

With tasks like geometry design, simulation setup, fatigue testing, and comparison against a baseline model, the initial project timeline was ambitious and comprehensive. Even though the initial goals were well-defined, some aspects—like the amount of time needed for mesh convergence studies or for assessing 12 design iterations—were understated. Furthermore, I did not initially anticipate the extent to which material stiffness (TPU A85 vs. A95) would affect the outcomes; this factor ultimately became a key component of the investigation. In hindsight, it would have been advantageous to include additional buffer time for the setup of the parametric simulation and for the post-processing outcomes.

In general, the team's task allocation was reasonable and fair, considering the interests and strengths of each individual. While others worked on the upper platform, prismatic link, universal joint, and gait planning, I concentrated on the end effector. Sometimes there was overlap, like making sure my design worked with the prismatic link, but roles were explained clearly, and we kept a shared folder for feedback and geometry handovers. The workload did, however, somewhat change in the later stages, especially when certain team members

experienced delays. Because of this, I occasionally helped with geometry alignment or advised on simulation setups that were outside of my purview. Even though it momentarily increased my workload, this was necessary to guarantee seamless subsystem integration.

Our project management process relied heavily on team meetings. Every week, we got together to talk about obstacles, assess our progress, and make plans for the future. We were able to promptly address problems like component geometry interference and simulation assumption misalignment thanks to these meetings. We were able to work together even though we were working asynchronously, thanks to communication tools like Microsoft Teams and shared OneDrive folders. We had to adjust our internal deadlines to deal with the issue of some tasks taking longer than anticipated, especially the initial FEA setup and mesh convergence validation.

I learnt a lot about overseeing technical tasks and collaborating with a multidisciplinary team while working on this project. I discovered that flexibility is crucial because a project needs to change over time, and sticking to original plans can backfire. Additionally, I gained a greater understanding of the value of documentation and version control, particularly when testing several geometries and simulations simultaneously. In terms of collaboration, I found that managing big projects with many moving components requires strong leadership, even if it is informal.

I would recommend establishing a team lead sooner and incorporating a systematic risk assessment into our planning stage if I were to redo the project. To prevent late-stage integration problems, we should have also specifically designated a team member to supervise geometry compatibility between subsystems. To lower uncertainty, it would also be beneficial to incorporate validation benchmarks earlier in the design cycle, possibly through faster simulation approximations or low-fidelity physical testing.

Even though some adjustments were required along the way, I think the group and I ultimately met the main goals. Target performance metrics were met by the end effector design, and the system's multifunctional and terrain-adaptive objectives were reinforced by its incorporation into the hexapod robot. Future students working on a similar group project should stay adaptable, keep thorough records, and communicate often, in my opinion. Collaboration and flexibility are just as important to project success as technical precision.

